Journal of the Korean Crystal Growth and Crystal Technology
Vol. 28, No. 1 (2018) 44-50
https://doi.org/10.6111/JKCGCT.2018.28.1.044

p-ISSN 1225-1429
e-ISSN 2234-5078

Improved high-performance $La_{0.7}Sr_{0.3}M_xFe_{1-x}O_3$ (M = Cu, Cr, Ni) perovskite catalysts for ortho-para hydrogen spin conversion

Jeong-Gil Choi†, Euiji Choi*, Soon-Cheol Kweon** and In-Hwan Oh**

Department of Chemical Engineering and Advances Materials, Hannam University, Taejon 34430, Korea
**Applied Chemistry, Department of Materials Science and Engineering, Kyushu University, Fukuoka, 819-0395, Japan*
***Green City Technology Institute, Korea Institute of Science and Technology, Seoul 02792, Korea*

(Received December 4, 2017)
(Revised December 23, 2017)
(Accepted December 28, 2017)

Abstract The improved high-performance Fe-based perovskite-type oxides ($La_{0.7}Sr_{0.3}M_xFe_{1-x}O_3$, M = Cu, Cr, Ni) were synthesized by a citrate method and characterized by SEM, EDS, XRD and NMR spectroscopy analyses. The characterization analyses revealed that the stoichiometric amounts of lattice oxygen were existed in all of perovskite samples except for a nickel-doped perovskite. Fe-based perovskites exhibited a surprising result for ortho-para H_2 spin conversion reaction, indicating two orders of magnitude higher conversions and conversion rates than commercial Fe_2O_3. It was considered that this conversion difference might be attributed to the presence of oxygen vacancies in Fe-based perovskites prepared in this study.

Key words $La_{0.7}Sr_{0.3}M_xFe_{1-x}O_3$ (M = Cu, Cr, Ni) perovskites, Commercial Fe_2O_3 catalyst, Ortho-para hydrogen spin conversion, Particle size, Structure sensitivity

1. Introduction

Recently, there is a growing interest in the use of hydrogen since hydrogen has become one of the primary sustainable energy resources to minimize air pollution, green-house gas production, and global energy crisis, especially through transportation and power generation. For instance, in the sector of green transportation using fuel cell vehicle, the compressed hydrogen storage has been on the verge of utilizing commercially available hydrogen storage technologies. Up to a maximum of 700 bar (~10,000 psi), the modest amount of hydrogen can be stored for urban transportation in short period of time. However, for the compressed hydrogen storage there are the main disadvantages which are related to the low volumetric energy density and safety concern. Zhang et al. reported that liquid hydrogen storage could be one of the possible solutions for overcoming these difficulties [1].

At this point, one might have to significantly consider the phase conversion process of ortho-hydrogen to para-hydrogen via metallic catalysts in order to fill liquid hydrogen into cryogenic fuel storage vessel as well as to maintain liquid hydrogen in liquid phase for the longer time [2, 3]. Until now, the iron (III) oxide (Fe_2O_3) has been widely used as a commercial catalyst for the ortho-para hydrogen spin conversion process. If some crystalline materials with comparatively higher conversion rate are successfully developed in the near future, it is expected that these could be used for future high compact liquid hydrogen storage in the application of unmanned aerial vehicle. For this purpose, as one of the strong candidates Fe-based perovskite-type oxides ($La_{0.7}Sr_{0.3}M_xFe_{1-x}O_3$) were suggested to be investigated.

Here, we report that Fe-based perovskite catalysts show reaction rates for ortho-para hydrogen conversion higher than commercial Fe_2O_3 catalyst. The Fe-based perovskite oxides have drawn particular interests because they can be easily prepared with catalytic properties which are superior to those of existing catalysts, by substituting a small fraction of dodecahedral A- and octahedral B-site atoms with other cations [4]. Previous investigation has been concentrated upon general chemical reactions such as oxidation, reduction, and reforming, etc. [5-7]. Inspite of extensive research work, no former studies have been reported for ortho-para hydrogen spin conversion over Fe-based perovskite catalysts.

Based on the above-mentioned background, we have synthesized a series of Fe-based perovskites ($La_{0.7}Sr_{0.3}M_xFe_{1-x}O_3$) with three different transition metals (M = Cu, Cr, Ni) using a citrate method. As the

†Corresponding author
E-mail: father8318@naver.com

characterizing tools, the SEM, EDS, XRD, and NMR spectroscopy techniques were employed to obtain the information concerning the surface morphology, elemental analysis, the crystallite size, and hydrogen spin conversion, respectively. Finally, the ortho-para hydrogen spin conversion reaction has been carried out so as to figure out the availability of Fe-based perovskites prepared in this study as catalysts, and compare these materials with a commercial Fe_2O_3 catalyst.

2. Experimental

2.1. Catalyst Synthesis

A series of Fe-based perovskites ($La_{0.7}Sr_{0.3}M_xFe_{1-x}O_3$) were prepared using the partial substitution of Fe with three different transition metals (M = Cu, Cr, Ni) by a citrate method [8-10]. The precursor was a solution of lanthanum, strontium, copper, chromium, nickel, and iron nitrates in stoichiometric proportion. The precursors used were citric acid anhydrous (99.5 %, Hayashi), lanthanum (III) nitrate hexahydrate (98 %, Samchun), strontium nitrate (98 %, Kanto), nickel (II) nitrate hexahydrate (98 % Samchun), copper (II) nitrate trihydrate (99 %, Hayashi), chromium (II) nitrate nonahydrate (98 % Kanto) and iron (III) nitrate nonahydrate (98.5 %, Samchun). The citric acid solution was prepared using a citric acid precursor and distilled water. An appropriate amount of lanthanum, strontium, iron, and other metal (M) nitrate precursors were mixed with distilled and deionized water, and stirred thoroughly. The initially prepared citric acid solution was added with the metal-nitrate precursor's solution. The precursor mixed solution was dried at 393 K for 16 h, and calcined at 1173 K for 6 h to obtain the final form of perovskites.

2.2. Catalyst Characterization

The specific surface areas were determined by the Brunauer-Emmett-Teller (BET) method with nitrogen at 77 K. A gas mixture containing 30 % nitrogen in He was used for standard single point BET surface area measurements.

The SEM images and EDS analyses of the samples were obtained using FE-SEM (HITACHI-S4200). A computer controlled Bruker D8 Advance rotating anode X-ray diffractometer was used for bulk characterization of the Fe-based perovskite oxides. The crystallite phase and size were determined using the CuK_α irradiation with two theta value of 20 to 60 degree with a scan rate of 2 degree per minute. The crystallite dimensions were obtained using the Scherrer equation, $D_p = 0.9\lambda/(B\cos\theta)$, where D_p is the crystal thickness, λ is the wave length of the X-radiation, B is the peak width corrected for instrumental broadening, and θ is the Bragg angle of the diffraction peak.

2.3. Catalytic Activity

The ortho-para hydrogen spin conversion was performed at 300 K using the prepared perovskite samples. Before the measurement of conversion, the powder sample was made into a pellet (diameter: 10 mm, thickness: 1 mm) using a pelletizer (Carver Lab. Press). About 0.15 g of each perovskite sample was used for measuring the reactivity. An inlet flow rate of normal hydrogen gas (99.99 %, DEO) was maintained at 40 ml/min by a mass flow controller (Bronkhost). The normal hydrogen gas was passed through the sample bed in the up-flow mode. The converted ortho-para hydrogen mixture was collected in a NMR glass sample tube. Before capturing the spin-converted hydrogen gas the NMR glass tube was evacuated with a vacuum pump (ULVAC-DA-60S). The total time to capture the converted gas was fixed for 3 minutes for each sample. The ortho-para hydrogen spin conversions were measured using an NMR spectrometer (BRUKER 400 MHz Ultra Shield). The software used to collect the spectra is Bruker Topsin 3.1. A solution of 1 % $CHCl_3$/Acetone-d_6 was used as standard for the gas phase NMR analysis. A blank run was performed without putting any sample in the reactor by flowing the hydrogen gas.

3. Results and Discussion

3.1. Physicochemical Properties of the Catalysts

The prepared Fe-based perovskite oxides show low surface areas ranging from 1.71 to 3.76 m^2/g (Table 1). These low surface areas are in good agreement with the literature [11, 12]. However, compared to the original material of $LaFeO_3$ perovskite ($S_g = 0.9\ m^2/g$) these materials have the higher surface areas, suggesting that Sr, Cu, Cr, and Ni might behave like a structural promoter. In fact, the atomic diameters of Sr, Cu, Cr, and Ni (= 0.4, 0.25, 0.28, and 0.27 nm, respectively) are significantly larger than that of oxygen (= 0.1 nm). It is generally known that surface areas for perovskite oxides are around two orders of magnitude lower than those of

Table 1
Sorption properties of Fe-based perovskite oxides[†]

	S_g (m^2/g)	D_p (nm)	D_c (nm)	$\Delta=(D_p - D_c/D_p) \times 100$ (%)	Crystalline phase
$La_{0.7}Sr_{0.3}FeO_3$	3.41	294	30.3	90	Polycrystalline
$La_{0.7}Sr_{0.3}Cu_{0.3}Fe_{0.7}O_3$	1.71	545	44.6	92	Polycrystalline
$La_{0.7}Sr_{0.3}Cr_{0.3}Fe_{0.7}O_3$	3.76	248	40.5	84	Polycrystalline
$La_{0.7}Sr_{0.3}Ni_{0.3}Fe_{0.7}O_3$	3.34	279	37.3	86	Polycrystalline

[†]S_g, D_p and D_c indicate the surface area, particle size, and crystallite size of the corresponding perovskite oxides, respectively.

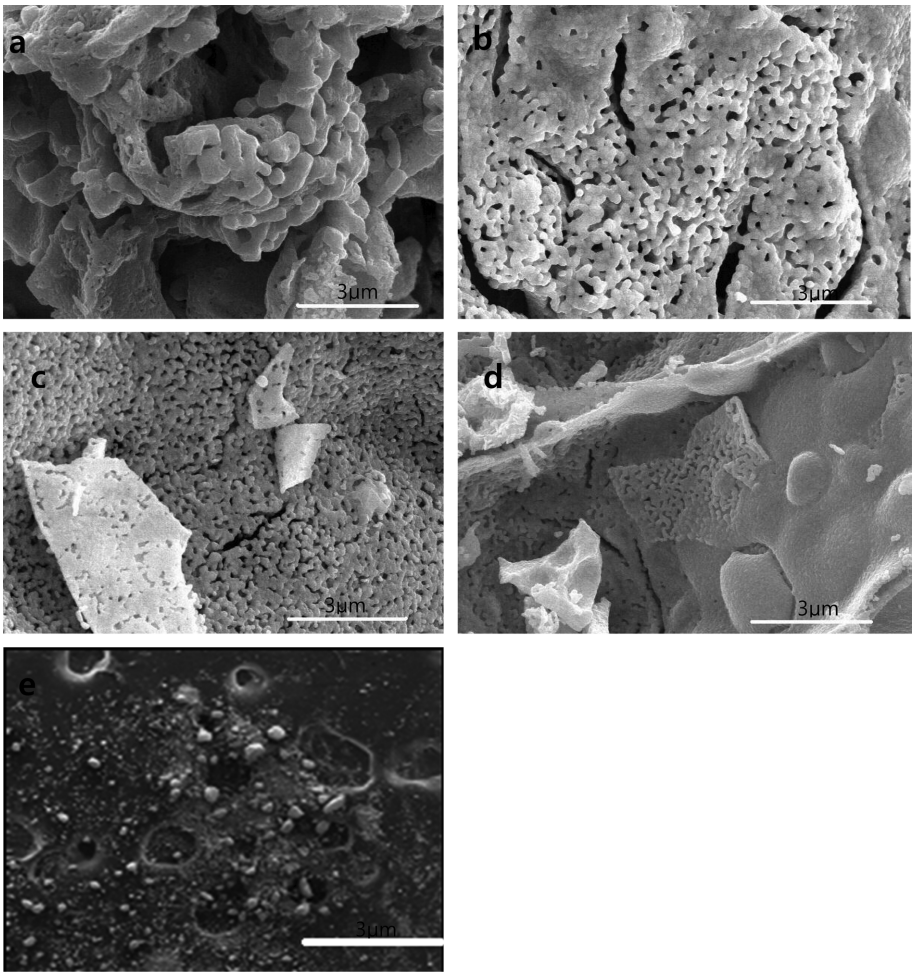

Fig. 1. SEM images of the synthesized catalysts: (a) $La_{0.7}Sr_{0.3}FeO_3$, (b) $La_{0.7}Sr_{0.3}Cu_{0.3}Fe_{0.7}O_3$, (c) $La_{0.7}Sr_{0.3}Cr_{0.3}Fe_{0.7}O_3$, (d) $La_{0.7}Sr_{0.3}Ni_{0.3}Fe_{0.7}O_3$, and (e) Commercial Fe_2O_3 catalyst.

typical oxides such as Al_2O_3 and CuO. The primary reason for the production of low surface areas is assumed to be the high preparation temperature (> 1,000 K) used during the calcination. For our Fe-based perovskite oxides, the final synthesis temperature and time for calcination was 1173 K and 6 h, respectively.

Table 1 also gives some of the structural features of the Fe-based perovskite oxides. For all of these materials the crystallites were much smaller than the particles. Recall that the particle sizes were based on the surface area, therefore they reflect average surface character as compared to the crystallite sizes reflecting average bulk character. Deviations between the crystallite and particle sizes for these catalysts suggested that the particles were polycrystalline.

As shown in Fig. 1, the SEM images of the prepared $La_{0.7}Sr_{0.3}M_xFe_{1-x}O_3$ (M = Cu, Cr, Ni) perovskites were obtained, and compared with the commercially available Fe_2O_3 sample (Ionex®-Type O-P catalyst, Molecular Products, Inc.). The analyses of the images revealed that the surface morphology of the Fe-based perovskites was changed with the addition of other transi-

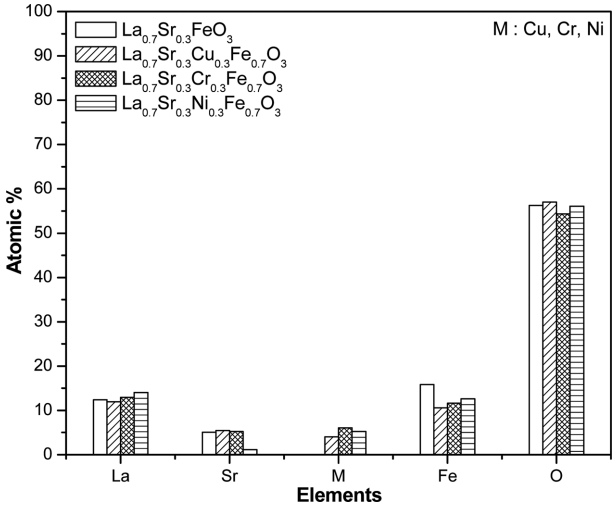

Fig. 2. EDS analyses of the metal (M: Cu, Ni, and Cr) impregnated $La_{0.7}Sr_{0.3}M_{0.3}Fe_{0.7}O_3$ samples.

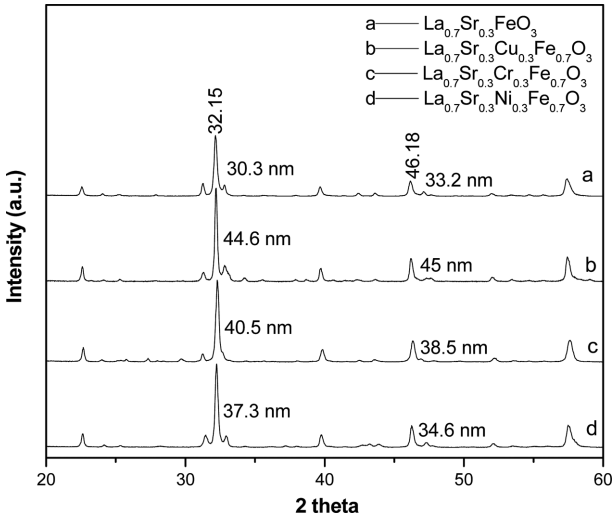

Fig. 3. X-ray diffraction patterns of (a) $La_{0.7}Sr_{0.3}FeO_3$, (b) $La_{0.7}Sr_{0.3}Cu_{0.3}Fe_{0.7}O_3$, (c) $La_{0.7}Sr_{0.3}Cr_{0.3}Fe_{0.7}O_3$, and (d) $La_{0.7}Sr_{0.3}Ni_{0.3}Fe_{0.7}O_3$.

tion metals in the perovskite phase. From Fig. 1(a, b), it can be seen that by the addition of copper in the Fe-based perovskite phase (shown in Fig. 1(a)), the surface morphology is uniformly distributed with the metal copper. Similar features were obtained for the chromium-impregnated sample. However, in the case of nickel-substituted sample a comparatively less porous and less crystalline phase was obtained.

The EDS patterns of all the prepared samples were obtained and the analysis of the elements present in each sample is shown in Fig. 2. The compositional analyses revealed that all of the Fe-based perovskites contained similar amounts of five different elements (La, Sr, M, Fe, O) within the experimental error range. It appeared that the stoichiometric amounts of lattice oxygen were existed in all the perovskite samples except for a nickel-doped perovskite (Table 2). The strontium element in this nickel-impregnated ($La_{0.7}Sr_{0.3}Ni_{0.3}Fe_{0.7}O_3$) sample was present in a relatively small amount, indicating the presence of non-stoichiometric large amount of lattice oxygen with the Sr/O ratio of 0.02. These results exhibit that the preparation of Fe-based perovskites is influenced by further addition of transition metals in the B site of perovskite structure. Fig. 3 shows the XRD patterns for the formation of the perovskite phases at $2\theta = 32.15$ and 46.18 degree, which is in good agreement with the literature [13]. We can see that the crystallite size is increased by the addition of transition metals. The smallest crystallite size of 37.3 nm at 32.15 degree was obtained for nickel-impregnated sample. In the meantime, the largest crystallite size of 44.6 nm was observed in copper-doped perovskite sample.

3.2. Activity of Fe-Based Perovskite Oxides

NMR analysis technique was utilized to investigate the reactivity of Fe-based perovskites for the non-dissociative ortho-para H_2 spin conversion (ortho → para hydrogen). In particular, the effect of other transition metals (M = Cu, Ni, Cr) impregnated in $La_{0.7}Sr_{0.3}M_xFe_{1-x}O_3$ perovskites on the reaction has also been scrutinized.

Table 2
Molar ratios of metal to oxygen in Fe-based perovskite oxides analyzed by EDS

	La/O	Sr/O	Fe/O	M/O[a]
$La_{0.7}Sr_{0.3}FeO_3$	0.22(0.23)[b]	0.09(0.10)	0.28(0.33)	-
$La_{0.7}Sr_{0.3}Cu_{0.3}Fe_{0.7}O_3$	0.21(0.23)	0.10(0.10)	0.19(0.33)	0.07(0.10)
$La_{0.7}Sr_{0.3}Cr_{0.3}Fe_{0.7}O_3$	0.24(0.23)	0.10(0.10)	0.21(0.33)	0.11(0.10)
$La_{0.7}Sr_{0.3}Ni_{0.3}Fe_{0.7}O_3$	0.25(0.23)	0.02(0.10)	0.23(0.33)	0.09(0.10)

[a]Metals (Cu, Cr, and Ni) corresponding to three Fe-based perovskite samples of $La_{0.7}Sr_{0.3}Cu_{0.3}Fe_{0.7}O_3$, $La_{0.7}Sr_{0.3}Cr_{0.3}Fe_{0.7}O_3$, and $La_{0.7}Sr_{0.3}Ni_{0.3}Fe_{0.7}O_3$.
[b]Values in parenthesis indicating stoichiometric molar ratios of metal to oxygen.

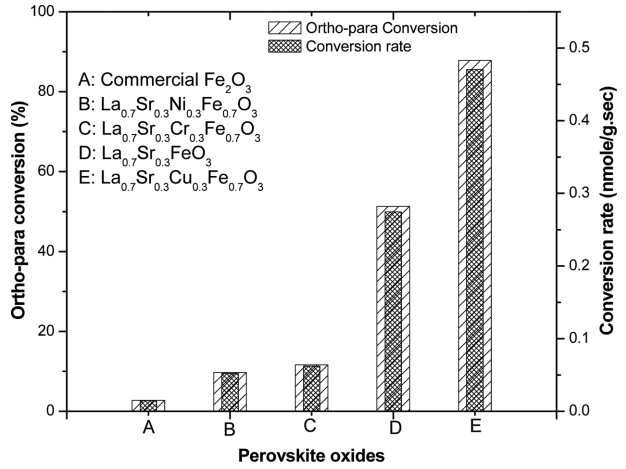

Fig. 4. Ortho-para conversion and the conversion rate of the prepared catalysts: (a) Commercial Fe_2O_3 catalyst (b) $La_{0.7}Sr_{0.3}Ni_{0.3}Fe_{0.7}O_3$, (c) $La_{0.7}Sr_{0.3}Cr_{0.3}Fe_{0.7}O_3$, (d) $La_{0.7}Sr_{0.3}FeO_3$, and (e) $La_{0.7}Sr_{0.3}Cu_{0.3}Fe_{0.7}O_3$.

The ortho-para hydrogen spin conversion and the conversion rate expressed on a per gram basis are shown in Fig. 4. The peak of ortho hydrogen present in the normal hydrogen is located at 5.069 ppm, which is consistent with the previous studies [14-16]. It can be seen that the ortho hydrogen was effectively converted to para hydrogen in presence of commercial Fe_2O_3 and Fe-based perovskites.

Amongst different perovskite oxides, copper-doped perovskite in the B site exhibited the highest conversion (88 %) while nickel-impregnated perovskite showed the lowest conversion (12 %). A plausible explanation for the difference in conversion is that the reaction rate is directly correlated with the particle size (Table 1). It is generally known that the ortho-para hydrogen spin conversion is not a chemical reaction but a magneto-catalytic reaction [17], which is accelerated by a magnetic susceptibility leading to paramagnetism (Pr_2O_3, Nd_2O_3, Sm_2O_3), antiferromagnetism (Cr_2O_3, CoO) or ferromagnetism (Fe_2O_3, EuO) [17, 18]. However, for hydrogen spin conversion process the hydrogen should adsorb on the surface of the materials as the first step. Therefore, it is also important to consider the bulk and surface properties of catalysts such as particle size and material composition. For example, as shown in Fig. 3, the highest conversion rate of $La_{0.7}Sr_{0.3}Cu_{0.3}Fe_{0.7}O_3$ perovskite might be ascribed to the production of the largest particle size (545 nm).

The ortho-para hydrogen conversion for the perovskite oxides prepared in the current study is linearly related to the particle size. The conversion difference could be interpreted in terms of differing bonding geometries at particle surfaces. Recall that the Fe-based perovskite oxides are polycrystalline particles. The presence of polycrystalline particles indicates that the cracks, kinks, and grain boundaries were generated at surfaces during the formation of perovskites, which can be favorably used for catalytic reactions [19].

Based on the presence of the linear relationship between the particle size and reaction rate, we concluded that the ortho-para hydrogen spin conversion reaction over Fe-based perovskite oxides was structure-sensitive. It is noted that the concept of structure sensitivity could be described in two aspects: the bulk and surface viewpoints. One bulk aspect is associated with the relationship between the reaction rate and the particle size [20, 21]. In this case, the reaction rate should be linearly related to the particle size. The other surface aspect has been suggested by Choi et al. [22, 23] who used Mo nitrides and carbides for pyridine hydrodenitrogenation. They found that the activity changed with variation of surface properties over these materials. Based on these findings, they proposed that for materials like transition metal nitrides and carbides, the surface structure and stoichiometry should be taken into account for the application of structure sensitivity concept. This aspect would be the next topic of investigation for ortho-para hydrogen spin conversion over Fe-based perovskite catalysts. Therefore, it might be appropriate for our system of Fe-based perovskites to be considered as a structure-sensitive reaction.

Since no previous investigation has, thus far, been reported for ortho-para hydrogen spin conversion over Fe-based perovskite catalysts, we propose for the first time that the structure sensitivity can be applied for our system. Nonetheless, in order to better understand the hydrogen spin conversion difference between various Fe-based perovskites further works on magnetic and electronic properties are definitely needed.

3.3. Comparison Between Commercial Fe_2O_3 and Fe-Based Perovskite Oxides

Due to very limited information, it is interesting to compare the conversion rates on these perovskite oxides with those on commercial Fe_2O_3 catalysts. The Fe-based perovskites synthesized in this study showed as much as two orders of magnitude higher conversions and conversion rates than commercial Fe_2O_3 sample (rhombohedral structure). These perovskites reached a maximum conversion of 88 % while the commercial Fe_2O_3 catalyst showed a conversion of 3 %. Even though these

materials have different crystal structures, the primary reason for the conversion difference is the fact that these perovskites contain Sr as a promoter in the A site, and transition metals M (Cu, Cr, and Ni) in the B site of basic perovskite structure. It was considered that this divalent Sr was partially substituted for the trivalent La by 30 mol%, causing the charge imbalance in the A site to take place. This charge imbalance might have given rise to the production of oxygen vacancies, which resulted in the increase of the ortho-para hydrogen spin conversion. Likewise, it was expected that the similar electronic behavior might have happened in the B site.

The incorporations of Sr^{2+} into the A sites and $M^{\lambda+}$ into the B sites alter the physical and chemical properties of the perovskite oxide, such as the nonstoichiometry of lattice oxygen and the density of oxygen vacancies [11, 12]. For example, in our perovskite oxides the number of oxygen vacancies can be controlled by doping the different transition metals (such as Sr, Cr, Ni, and Cu) into ABO_3 structure. The presence of oxygen vacancies is one of the key criteria to obtain the good catalytic performance. Kim et al. reported that the conversion for NO oxidation increased by a maximum of 86 % using $La_{0.9}Sr_{0.1}CoO_3$ catalyst compared to $LaCoO_3$ catalyst [11]. They explained that the increase of conversion was ascribed to the presence of charge imbalance generated by the partial substitution of a La^{3+} ion with a Sr^{2+} ion (10 mole%). The oxidation states of elements in our perovskite oxides are shown in Table 3. Depending on the oxidation states of elements, the value of δ was determined and located between 0.15 and 0.8 in $La_{0.7}Sr_{0.3}M_xFe_{1-x}O_{3-\delta}$, indicating the existence of oxygen vacancies.

All in all, this new class of Fe-based perovskite oxides with the high catalytic performance and the advantageous reconfiguration of electronic structure would open up new opportunities for catalytic applications, especially in ortho-para hydrogen spin conversion reaction.

4. Conclusions

We have investigated a series of Fe-based perovskite-type oxides ($La_{0.7}Sr_{0.3}M_xFe_{1-x}O_3$) which were doped by different transition metals (M = Cu, Cr, Ni). The stoichiometric amounts of lattice oxygen were existed in all the perovskite samples except for a nickel-doped perovskite, and the largest crystallite size of 44.6 nm was obtained for $La_{0.7}Sr_{0.3}Cu_{0.3}Fe_{0.7}O_3$ perovskite phase. It was proved that Fe-based perovskites were active for ortho-para hydrogen spin conversion. The conversions of these materials was as much as 30 times higher than that of Fe_2O_3 sample, which is due to the presence of oxygen vacancies in Fe-based perovskites prepared in the current study. There is a linear relationship between the hydrogen conversion and the particle size of these perovskite oxides.

Table 3
Oxidation states of elements in Fe-based perovskite oxides

Sample	Oxidation states of elements					
$La_{0.7}Sr_{0.3}FeO_3$	$La^{2.1+}$	$Sr^{0.6+}$	-	Fe^{3+}	$O^{5.7-}$	$\delta = 0.15^a$
$La_{0.7}Sr_{0.3}FeO_3$	$La^{2.1+}$	$Sr^{0.6+}$	-	Fe^{2+}	$O^{4.7-}$	$\delta = 0.65$
$La_{0.7}Sr_{0.3}Cu_{0.3}Fe_{0.7}O_3$ (For Cu^{2+} and Fe^{3+})	$La^{2.1+}$	$Sr^{0.6+}$	$Cu^{0.6+}$	$Fe^{2.1+}$	$O^{5.4-}$	$\delta = 0.30$
$La_{0.7}Sr_{0.3}Cu_{0.3}Fe_{0.7}O_3$ (For Cu^{2+} and Fe^{2+})	$La^{2.1+}$	$Sr^{0.6+}$	$Cu^{0.6+}$	$Fe^{1.4+}$	$O^{4.7-}$	$\delta = 0.65$
$La_{0.7}Sr_{0.3}Cu_{0.3}Fe_{0.7}O_3$ (For Cu^{1+} and Fe^{3+})	$La^{2.1+}$	$Sr^{0.6+}$	$Cu^{0.3+}$	$Fe^{2.1+}$	$O^{5.1-}$	$\delta = 0.45$
$La_{0.7}Sr_{0.3}Cu_{0.3}Fe_{0.7}O_3$ (For Cu^{1+} and Fe^{2+})	$La^{2.1+}$	$Sr^{0.6+}$	$Cu^{0.3+}$	$Fe^{1.4+}$	$O^{4.4-}$	$\delta = 0.80$
$La_{0.7}Sr_{0.3}Cr_{0.3}Fe_{0.7}O_3$ (For Cr^{3+} and Fe^{3+})	$La^{2.1+}$	$Sr^{0.6+}$	$Cr^{0.9+}$	$Fe^{2.1+}$	$O^{5.7-}$	$\delta = 0.15$
$La_{0.7}Sr_{0.3}Cr_{0.3}Fe_{0.7}O_3$ (For Cr^{3+} and Fe^{2+})	$La^{2.1+}$	$Sr^{0.6+}$	$Cr^{0.9+}$	$Fe^{1.4+}$	$O^{5.0-}$	$\delta = 0.50$
$La_{0.7}Sr_{0.3}Ni_{0.3}Fe_{0.7}O_3$ (For Ni^{2+} and Fe^{3+})	$La^{2.1+}$	$Sr^{0.6+}$	$Ni^{0.6+}$	$Fe^{2.1+}$	$O^{5.4-}$	$\delta = 0.30$
$La_{0.7}Sr_{0.3}Ni_{0.3}Fe_{0.7}O_3$ (For Ni^{2+} and Fe^{2+})	$La^{2.1+}$	$Sr^{0.6+}$	$Ni^{0.6+}$	$Fe^{1.4+}$	$O^{4.7-}$	$\delta = 0.65$

[a]Calculated from the actual structure of $La_{0.7}Sr_{0.3}M_xFe_{1-x}O_{3-\delta}$ for Fe^{2+}, Fe^{3+}, Cu^{1+}, Cu^{2+}, Cr^{3+} and Ni^{2+}.

Acknowledgements

Professor Choi appreciates Hannam University for supporting during the period starting from April 1, 2017 through March 31, 2018.

References

[1] J. Zhang, T.S. Fisher, P.V. Ramachandran, J.P. Gore and I. Mudawar, "A review of heat transfer issues in hydrogen storage technologies", J. Heat Transfer. 127 (2005) 1391.
[2] K. Makoshi, M. Rami and E. Ilisca, "Dipolar and contact processes in H_2 o-p conversion on ionic surfaces", J. Physics: Condensed Matter. 5 (1993) 7325.
[3] M. Rami, K. Makoshi and E. Illisca, "Physisorption and ortho-para conversion of molecular hydrogen on solid surfaces", Appl. Surf. Sci. 68 (1993) 197.
[4] S.K. Dickinson Jr., "The chemical structure of solids", AF CRL-70-0727, National Technical Information Center (1970).
[5] B. Michael and S. McIntosh, "Kinetics of ortho-para conversion of hydrogen", J. Catal. 255 (2008) 313.
[6] F. Dhainaut, S. Pietrzyk and P. Granger, "Kinetic investigation of the NO reduction by H_2 over noble metal based catalysts", Catal. Today 119 (2007) 94.
[7] S.Q. Chen and Y. Liu, "$LaFe_yNi_{1-y}O_3$ supported nickel catalysts used for steam reforming of ethanol", Int'l. J. of Hydrogen Energy 34 (2009) 4735.
[8] M.M. Natile, F. Poletto, A. Galenda, A. Glisenti, T. Montini, L. De Rogatis and P. Fornasiero, "$La_2Cu_{0.8}Co_{0.2}O_{4+}$ by Pechini method", Chem. Mat'ls 20 (2008) 2314.
[9] E. Arendt, A. Maione, A. Klisnska, O. Sanz, M. Montes, S. Suarez, J. Blanco and P. Ruiz, "High-efficiency $CeWO_x$ catalyst for the selective catalytic reduction of NO_x with NH_3", Appl. Catal. A: General 339 (2008) 1.
[10] D.H. Prasad, S.Y. Park, E.O. Oh, H. Ji, H.R. Kim, K.J. Yoon, J.W. Son and J.H. Lee, "Synthesis of nano-crystalline $La_{1-x}Sr_xCoO_{3-\delta}$ perovskite oxides by EDTA-citrate complexing process and its catalytic activity for soot oxidation", Appl. Catal. A; General 447 (2012) 100.
[11] C.H. Kim, G. Qi, K. Dahlberg and W. Li, "Strontium-doped perovskites rival platinum catalysts for treating NO_x in simulated diesel exhaust", Science 327 (2010) 1624.
[12] J. Suntivich, K.J. May, H.A. Gasteiger, J.B. Goodenough and Y. Shao-Horn, "A perovskite oxide optimized for oxygen evolution catalysis from molecular orbital principles", Science 334 (2011) 1383.
[13] J. Faye, A. Baylet, M. Trentesaux, S. Royer, F. Dumeignil, D. Duprez, S. Valange and J.M. Tatibouet, "Influence of lanthanum stoichiometry in $La_{1-x}FeO_{3-\delta}$ perovskites on their structure and catalytic performance in CH_4 total oxidation", Applied Catalysis B: Environment 126 (2012) 134.
[14] A. Gamliel, H. Allouche-Arnon, R. Nalbandian, C.M. Barzily, J.M. Gomori and R. Katz-Brull, "An apparatus for production of isotopically and spin-enriched hydrogen for induced polarization studies", Appl. Magnet. Reson. 39 (2010) 329.
[15] E. Sartori, M, Ruzzi, R.G. Lawler and N.J. Turro, "Demonstration of a chemical transformation inside a fullerene. The reversible conversion of the allotropes of $H_2@C_{60}$", JACS 130 (2008) 12752.
[16] J.G. Vitillo, L. Regli, S. Chavan, G. Ricchiardi, G. Spoto, P.D.C. Dietzel, S. Bordiga and A. Zecchina, "Role of exposed metal sites in hydrogen storage in MOFs", JACS 130 (2008) 8386.
[17] E. Baron and P.W. Selwood, "Parahydrogen conversion and magnetocatalytic effects over yttria and lutetia", J. Catal. 28 (1973) 422.
[18] C.F. Ng and P.W. Selwood, "Magnetic effects on the *ortho-para* hydrogen conversion over α-Cr_2O_3, CoO, and MnO", J. Catal. 43 (1976) 252.
[19] J.G. Choi, R.L. Curl and L.T. Thompson, "Molybdenum nitride catalysts: I. Influence of the synthesis factors on structural properties", J. Catal. 146 (1994) 218.
[20] G.A. Somorjai and J. Carrazza, "Structure sensitivity of catalytic reactions", Ind. Eng. Chem. Fund. 25 (1986) 63.
[21] M. Boudart, "Catalysis by supported metals", Princeton Univ. Press 1992: chap. 5.
[22] J.G. Choi, J.R. Brenner, C.W. Colling, K. Demczy, J.L. Dunning and L.T. Thompson, "Synthesis and characterization of molybdenum nitride hydrodenitrogenation catalysts", Catal. Today 15 (1992) 201.
[23] J.G. Choi, J.R. Brenner and L.T. Thompson. "Pyridine hydrodenitrogenation over molybdenum carbide catalysts", J. Catal. 154 (1995) 33.